Journal of Computational Applied Mechanics 2024, 55(3): 369-380

DOI: 10.22059/JCAMECH.2024.374760.1033

RESEARCH PAPER

Contribution study on factors impacting the vibration behavior of functionally graded nanoplates

H. Benaddi [a], B. Rebai [a], K. Mensouri [b], N. M. Seyam [c], A. M. Zenkour [d,e,*]

[a] *Faculty of Sciences & Technology, Civil Eng Department, University Abbes Laghrour, Khenchela 40000, Algeria*
[b] *Faculty of Sciences & Technology, Mechanic Eng Department, University Abbes Laghrour, Khenchela 40000, Algeria*
[c] *Department of Mathematical Sciences, College of Applied Sciences, Umm Al-Qura University, Makkah, Saudi Arabia*
[d] *Department of Mathematics, Faculty of Science, King Abdulaziz University, P.O. Box 80203, Jeddah 21589, Saudi Arabia*
[e] *Department of Mathematics, Faculty of Science, Kafrelsheikh University, Kafrelsheikh 33516, Egypt*

Abstract

This comprehensive study investigates the behavior of functionally graded (FG) nanoplates, providing insights into their characteristics and important design considerations. By examining factors such as homogenization models (Voigt Reuss, LRVE, and Tamura), volume fraction laws (power-law model, Viola-Tornabene four-parameter model, trigonometric model), eigenmode, aspect ratios, index material, and small-scale length parameters, the study evaluates their influence on the natural frequency response of simply supported nanoplates. A novel twisting function is introduced and its accuracy in predicting natural frequencies in FG square nanoplates is rigorously validated through numerical comparisons with existing literature. The findings obtained from this research offer valuable guidance for optimizing the design of FG nanoplates and significantly contribute to advancing our understanding of their dynamics and practical applications.

Keywords: Functionally graded materials; small-scale length parameter; homogenization models; volume fraction laws; vibrational behavior.

1. Introduction

Functionally graded materials (FGMs) have garnered significant attention due to their unique composition, characterized by gradually varying volume fractions of constituents to create specific profiles. These materials offer advantages such as effective resistance against high temperatures and reduced thermal stresses [1]. The distribution functions of FGMs play a crucial role in determining volume fraction profiles and material gradation, enabling tailored properties for specific applications. Nanotechnology has played a pivotal role in advancing FGMs by facilitating the fabrication and manipulation of nano-systems, nano-devices, and nanostructures at the molecular level. Notable contributions to this progress have been made by nano-materials like Carbon nanotubes (CNT), Graphene, Fullerene, and Quantumdots [2]. The incorporation of these nanostructures into nano-composites has resulted in multifunctional capabilities and applications in critical systems.

The thermal and electrical properties of FG nanoplates have also found applications in energy storage devices, including batteries and fuel cells, contributing to the advancement of sustainable energy solutions. Moreover, the micro/nanoelectromechanical systems (MEMS/NEMS) industry has embraced FG nanoplates as essential components in sensors, actuators, and resonators, leveraging their unique characteristics to push the boundaries of miniaturization

* Corresponding author. Tel.: +966-054-005-5690.
E-mail address: zenkour@kau.edu.sa

and performance [3-6].

Notably, FG nanoplates have emerged as promising candidates for thermal barrier coatings in high-temperature environments, such as turbine blades and jet engines, where their ability to withstand extreme conditions is invaluable. Furthermore, the biocompatibility and tailored mechanical properties of these nanoplates have opened doors to their utilization in biomedical implants and prosthetics, offering solutions that seamlessly integrate with the human body.

The study of FG nanoplates has unveiled a realm of practical applications that span across diverse fields, from aerospace and automotive to biomedical and energy industries. These advanced nanostructures boast unique advantages stemming from their meticulously tailored material properties, enabling efficient thermal management, enhanced structural integrity, and unparalleled mechanical performance.

The study of functional gradation in nano-material behavior is an intriguing area of materials analysis. FGMs have been extensively reviewed and applied in various structures and systems [7]. Researchers have explored the mechanics of FG materials and structures [8-18] and investigated functional gradation in different nanomaterial systems. For instance, recent developments have focused on NL-SG media [19], vibration of FG nanobeams accounting for shear deformation [20], linear free vibration of axially rotating FG microbeams [21], post-buckling behavior of FG nanobeams and bending analysis of an FG beam due to modified SG theory [22, 23]. These studies contribute to our understanding and analysis of functional gradation in nano-material systems and structures.

Various scientific theories and studies have emerged recently to explore the mechanical response of micro- and nanostructures, aiming to capture their unique characteristics and phenomena. Another significant theory is the Surface Elasticity Theory (SET), proposed by Thai et al. [24], which investigates surface effects on the analysis of nanoscale materials. Strain Gradient Theory (SGT), established by Ebrahimi et al. [25], focuses on the gradient of strain to describe material behavior. Additionally, the Nonlocal Elasticity Theory (NET), studied by various researchers [2, 26], takes into account nonlocal effects to examine the bending, buckling, and vibration of nanobeams and nano-plates. Notably, Reddy et al. [27, 28] examined the application of NET in investigating nanobeams and carbon nanotubes. Other studies have explored different aspects, including linear and nonlinear free vibration of FG nanobeams [29, 30], the combination of NET and MCST for analyzing static stability and vibration of nanostructures [31], and the analysis of porous FG nanobeams and nanoplates [32, 33]. These works provide valuable insights into the response of micro- and nanostructures, contributing to the advancement of our understanding of these fascinating systems.

This study aims to shed light on the behavior of FG nanoplates and provide insights into various factors influencing their natural frequency response. Factors such as homogenization models (including Voigt Reuss, LRVE, and Tamura), volume fraction laws (power-law model, Viola-Tornabene four-parameter model, trigonometric model), eigenmode, aspect ratios, index material, and small-scale length parameters were investigated. One of the key contributions of this study is the introduction of a novel twisting function, which was rigorously validated through numerical comparisons with existing literature. The accuracy of the twisting function in predicting natural frequencies in FG square nano-plates was confirmed, enhancing the reliability of the study. Through comparative analysis and validation, the research demonstrates the precision and dependability of the conducted numerical analysis. The results affirm the influence of factors such as thickness ratio, homogenization models, volume fraction laws, nonlocal parameter, eigenmode, aspect ratios, and index material on the natural frequency of nanoplates.

These findings offer valuable insights and guidance for optimizing the design of FG nanoplates. By considering the appropriate homogenization model, volume fraction law, and other identified factors, engineers and researchers can make informed decisions to enhance the natural frequency response of FG nanoplates. Overall, this research significantly contributes to advancing our appreciative of FG nanoplate dynamics and their practical applications, enriching the knowledge in the field of nanoplate vibrations and providing a foundation for further exploration and optimization of FG nanoplate designs.

2. Nonlocal elasticity Eringen theory

Eringen proposed a concept stating that stress distribution within an elastic material is influenced not only by strain at a specific point but also by strains at all other points within the body. The nonlocal stress field can be mathematically stated as an integral involving the product of nonlocal modulus and classical macroscopic stress tensor, considering the entire volume of the material [34-37].

Furthermore, Eringen demonstrated that the nonlocal constitutive equation can also be signified in an alternative differential form. This formulation involves Laplacian operator acting on stress tensor [38], where a material constant τ is associated with internal and external characteristic lengths

$$(1 - \tau^2 L^2 \nabla^2)\sigma = t, \tag{1}$$

$$\tau^2 = \frac{\mu}{L^2} = \left(\frac{e_0 \bar{a}}{L}\right)^2, \tag{2}$$

where e_0 denotes a material constant and $\bar{a}$ and L are internal and external characteristic lengths.

3. Problem definition geometry

The problem supposes that the domain has the geometry of a nanoplate, shown in Figure 1, with a thickness of h, a length of a, and a width of b.

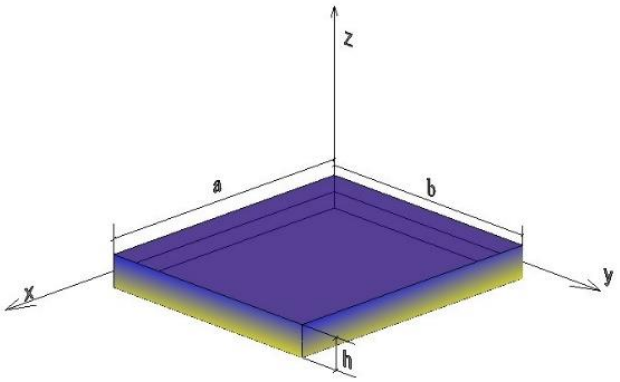

Figure 1: Geometry of an FG nanoplate.

The upper surface of the plate consists of a ceramic-rich material Si_3N_4 while lower surface is made of a metal-rich material SUS_{304}. The material properties, including mass density ρ and Young's modulus E, are determined as: $\rho_c = 2370$ kg/m^3 for Si_3N_4 and $\rho_m = 8166$ kg/m^3 for SUS_{304}; $E_c = 348.43$ N/m^2 and $E_m = 201.04$ N/m^2; Poisson's ratio v is supposed to be constant at 0.3.

In the case of FG structures, the predominant composition involves two phases with gradual variations in their volume fractions. As a result, the selection of appropriate formulas to determine the distribution of material constituents in these structures holds great importance. Presented below are some of the most applicable formulas for achieving material gradation in FGMs.

3.1. Power-law model

$$V_1 = \left(\frac{1}{2} + \frac{z}{h}\right)^p, \tag{3}$$

where p is the material index.

3.2. Trigonometric model

$$V_1 = \sin^2\left(\frac{1}{2} + \frac{z}{h}\right)^p . \tag{4}$$

3.3. Viola-Tornabene four-parameter model

$$V_1 = \left[1 - a\left(\frac{1}{2} - \frac{z}{h}\right) + b\left(\frac{1}{2} + \frac{z}{h}\right)^c\right]^p, \tag{5}$$

where a, b, and c are constants that state the material propagation in the FG plate.

4. Different micromechanics models

The micromechanics models preferred for comparison study are [39, 40]:

4.1. Mixture law (Voigt model)

Mixture law - Voigt model - is a mathematical model that describes the behavior of a composite material [41]

$$P(z) = P_c V(z) + P_m\big(1 - V(z)\big). \tag{6}$$

4.2. Reuss model

The Reuss model is a mathematical model used to calculate the effective properties of a composite material [42].

$$P(z) = \frac{P_c P_m}{P_c(1-V(z))+P_m V(z)}. \tag{7}$$

4.3. Tamura model

The method of Tamura is represented as [43, 44]

$$P(z) = \frac{(1-V(z))\,P_m(q-P_c)+V(z)\,P_c}{P_c(1-V(z))+P_m V(z)(1-V(z))\,(q-P_c)+V(z)\,P_c(q-P_m)}. \tag{8}$$

where q is the empirical term "stress-to-strain transfer" [45].

4.4. Mori-Tanaka model

The Mori–Tanaka method is represented by [46]

$$P(z) = P_m + \frac{V(z)\,(P_c-P_m)}{1+\frac{(1-V(z))(3P_c-P_m)}{3P_m+4}}, \tag{9}$$

where $P(z)$ denotes effective material property; P_m and P_c represent properties of the metal and ceramic faces of the plate.

4.5. Description by a representative volume element (LRVE)

The LRVE method is formulated under hypothesis that microstructure of heterogeneous material is known. In deterministic micromechanical framework, the LRVE requires input in the form of volume averages or ensemble averages of descriptors of the microstructures.

By employing LRVE method [43], the effective property is expressed as follows

$$P(z) = P_m\left(+\frac{V(z)}{\frac{1}{1-\frac{P_m}{P_c}}-\sqrt[3]{V(z)}}\right). \tag{10}$$

4.6. The displacement field

The theoretical change is determined according to three assumptions: the distribution in the plane and its transformation into material bending and shear, the similarity of plane bending changes to the classical plate theory, and the difference between shear strain. It is caused by shear stress, it disappears at the top and bottom of the plate. The resulting displacement field is then given byovided

$$\begin{aligned} u(x,y,z,t) &= u_0(x,y,t) - z\frac{\partial w_b}{\partial x} - f(z)\frac{\partial w_s}{\partial x}, \\ v(x,y,z,t) &= v_0(x,y,t) - z\frac{\partial w_b}{\partial y} - f(z)\frac{\partial w_s}{\partial y}, \\ w(x,y,z,t) &= w_b(x,y,t) + w_s(x,y,t), \end{aligned} \tag{11}$$

where $f(z)$ is the new formulation that has been used to express the warping function

$$f(z) = \left[\ln\left(\pi\, \mathrm{e}^{\frac{1}{20}}\right) - \frac{1}{10}(\mathrm{e}^{\pi z} + \mathrm{e}^{-\pi z})\right] z + \frac{1}{2}\ln\left(\pi\, \mathrm{e}^{\frac{1}{20}}\right) - \frac{2}{10}\cosh\left(\frac{\pi}{2}\right), \tag{12}$$

with $g(z) = \frac{\mathrm{d}}{\mathrm{d}z} f(z)$.

4.7. The nonlocal constitutive relations

The 2D nonlocal constitutive formulae for elastic FG nanoplate are represented by

$$\begin{Bmatrix} \sigma_x \\ \sigma_y \\ \tau_{yz} \\ \tau_{xz} \\ \tau_{xy} \end{Bmatrix} - \mu\left(\frac{\partial^2}{\partial x^2} + \frac{\partial^2}{\partial y^2}\right)\begin{Bmatrix} \sigma_x \\ \sigma_y \\ \tau_{yz} \\ \tau_{xz} \\ \tau_{xy} \end{Bmatrix} = \begin{bmatrix} C_{11} & C_{12} & 0 & 0 & 0 \\ C_{12} & C_{22} & 0 & 0 & 0 \\ 0 & 0 & C_{44} & 0 & 0 \\ 0 & 0 & 0 & C_{55} & 0 \\ 0 & 0 & 0 & 0 & C_{66} \end{bmatrix}\begin{Bmatrix} \varepsilon_x \\ \varepsilon_y \\ \gamma_{yz} \\ \gamma_{xz} \\ \gamma_{xy} \end{Bmatrix}, \tag{13}$$

where $(\sigma_x, \sigma_y, \tau_{yz}, \tau_{xz}\ \tau_{xy})$ and $(\varepsilon_x, \varepsilon_y, \gamma_{yz}, \gamma_{xz}, \gamma_{xy})$ are stress and strain components. The stiffness coefficients C_{ij} are represnted by

$$C_{11} = C_{22} = \frac{E(z)}{1-v(z)^2},\quad C_{12} = \frac{vE(z)}{1-v(z)^2},\quad C_{44} = C_{55} = C_{66} = \frac{E(z)}{2[1+v(z)]}. \tag{14}$$

4.8 Hamilton's principle

Hamilton's principle is applied to derive the dymamic equations

$$0 = \int_0^t (\delta U - \delta K)\mathrm{d}t, \tag{15}$$

where δU and δK denote variation of strain and kinetic energies.

5. Solution procedure

Following Navier solution procedure, one supposes the following solute\on form for u_0, v_0, w_b and w_s that satisfies the boundary conditions

$$\begin{Bmatrix} u_0 \\ v_0 \\ w_b \\ w_s \end{Bmatrix} = \begin{Bmatrix} U_{mn}\cos(\alpha x)\sin(\beta y) \\ V_{mn}\sin(\alpha x)\cos(\beta y) \\ W_{bmn}\sin(\alpha x)\sin(\beta y) \\ W_{smn}\sin(\alpha x)\sin(\beta y) \end{Bmatrix} \mathrm{e}^{i\omega t}, \tag{16}$$

where U_{mn}, V_{mn}, W_{bmn} and W_{smn} are arbitrary parameters to be determined, ω is the eigenfrequency associated with (m,n)th eigenmode. The analytical solutions can be gained from

$$\left(\begin{bmatrix} a_{11} & a_{12} & a_{13} & a_{14} \\ a_{12} & a_{22} & a_{23} & a_{24} \\ a_{13} & a_{23} & a_{33} & a_{34} \\ a_{14} & a_{24} & a_{34} & a_{44} \end{bmatrix} - \lambda\omega^2 \begin{bmatrix} m_{11} & 0 & 0 & 0 \\ 0 & m_{22} & 0 & 0 \\ 0 & 0 & m_{33} & m_{34} \\ 0 & 0 & m_{34} & m_{44} \end{bmatrix} \right) \begin{Bmatrix} U_{mn} \\ V_{mn} \\ W_{bmn} \\ W_{smn} \end{Bmatrix} = \begin{Bmatrix} 0 \\ 0 \\ 0 \\ 0 \end{Bmatrix}, \tag{17}$$

with

$$\begin{gathered} a_{11} = A_{11}\alpha^2 + A_{66}\beta^2,\ \ a_{12} = \alpha\beta(A_{12} + A_{66}),\ \ a_{13} = -\alpha[B_{11}\alpha^2 + (B_{12} + 2B_{66})\beta^2], \\ a_{14} = -\alpha[B_{11}^s\alpha^2 + (B_{12}^s + 2B_{66}^s)\beta^2],\ \ a_{22} = A_{66}\alpha^2 + A_{22}\beta^2, \\ a_{23} = -\beta[(B_{12} + 2B_{66})\alpha^2 + B_{22}\beta^2],\ \ a_{24} = -\beta[(B_{12}^s + 2B_{66}^s)\alpha^2 + B_{22}^s\beta^2], \\ a_{33} = D_{11}\alpha^4 + 2(D_{12} + 2D_{66})\alpha^2\beta^2 + D_{22}\beta^4,\ \ a_{34} = D_{11}^s\alpha^4 + 2(D_{12}^s + 2D_{66}^s)\alpha^2\beta^2 + D_{22}^s\beta^4, \\ a_{44} = H_{11}^s\alpha^4 + 2(H_{12}^s + 2H_{66}^s)\alpha^2\beta^2 + H_{22}^s\beta^4 + A_{55}^s\alpha^2 + A_{44}^s\beta^2, \\ m_{11} = m_{22} = I_0,\ \ m_{33} = I_0 + I_2(\alpha^2 + \beta^2),\ \ m_{34} = I_0 + J_2(\alpha^2 + \beta^2), \\ m_{44} = I_0 + K_2(\alpha^2 + \beta^2),\ \ \lambda = 1 + \mu(\alpha^2 + \beta^2), \end{gathered} \tag{18}$$

in which (I_0, I_1, J_1, I_2, J_2, K_2) are mass inertias defined as

$$(I_0, I_2, J_2, K_2) = \int_{-h/2}^{h/2} (1,, z^2, zf, f^2)\rho(z)\mathrm{d}z, \tag{19}$$

and A_{ij}, B_{ij}, D_{ij}, etc., are the plate stiffness, defined by

$$\begin{gathered} \begin{Bmatrix} A_{11} & B_{11} & D_{11} & B_{11}^s & D_{11}^s & H_{11}^s \\ A_{12} & B_{12} & D_{12} & B_{12}^s & D_{12}^s & H_{12}^s \\ A_{66} & B_{66} & D_{66} & B_{66}^s & D_{66}^s & H_{66}^s \end{Bmatrix} = \int_{-h/2}^{h/2} C_{11}(1, z, f^2(z))\{v\}\mathrm{d}z, \\ (A_{22}, B_{22}, D_{22}, B_{22}^s, D_{22}^s, H_{22}^s) = (A_{11}, B_{11}, D_{11}, B_{11}^s, D_{11}^s, H_{11}^s), \\ A_{44}^s = A_{55}^s = \int_{-h/2}^{h/2} C_{44}[g(z)]^2\mathrm{d}z. \end{gathered} \tag{20}$$

6. Results and discussions

In this section, a numerical analysis is conducted to compare and validate the natural frequencies of square nanoplates with a gradient index of $p = 5$. The main goal is to assess the accuracy of the numerical outcomes attained here by comparing them with the findings presented in the literature by Natarajan et al. [22].

The nondimensionalized natural frequencies $\bar{\omega}$ are reported for all cases as follows:

$$\bar{\omega} = \omega h\sqrt{\frac{\rho_c}{G_c}}, \tag{21}$$

where ρ_c and G_c are mass density and shear modulus of the ceramic phase.

In their study, Natarajan et al. [22] employed the power law and Mori-Tanaka models. In our research, we extended their work by including additional homogenization models, such as Voigt, Reuss, LRVE, and Tamura, to investigate the natural frequencies of FG square nanoplates with a gradient index of $p = 5$.

Table 1. Comparative results of natural frequencies for square nanoplates with gradient index $p = 5$.

$f_1(z)$		Power-law model				Viola-Tornabene four-parameter model				Trigonometric model			
a/h	schemes	The nonlocal parameter μ				The nonlocal parameter μ				The nonlocal parameter μ			
		0	1	2	4	0	1	2	4	0	1	2	4
10	Mori-Tanaka [22]	0.0441	0.0403	0.0374	0.0330	0.0356	0.0325	0.0301	0.0267	0.0405	0.0370	0.0344	0.0304
	Voigt	0.0442	0.0401	0.0376	0.0331	0.0366	0.0337	0.0311	0.0274	0.0412	0.0374	0.0349	0.0309
	Reuss	0.0455	0.0418	0.0385	0.0339	0.0387	0.0353	0.0327	0.0288	0.0417	0.0381	0.0352	0.0312
	LRVE	0.0467	0.0425	0.0397	0.0350	0.0386	0.0351	0.0326	0.0287	0.0417	0.0380	0.0352	0.0312
	Tamura	0.0455	0.0418	0.0385	0.0339	0.041	0.0373	0.0347	0.0306	0.0429	0.0391	0.0365	0.0320
20	Mori-Tanaka [22]	0.0113	0.0103	0.0096	0.0085	0.0091	0.0083	0.0077	0.0068	0.0103	0.0094	0.0087	0.0077
	Voigt	0.0113	0.0104	0.0096	0.0084	0.0094	0.0085	0.0080	0.0074	0.0106	0.0096	0.0089	0.0078
	Reuss	0.0118	0.0107	0.0099	0.0087	0.0098	0.0090	0.0084	0.0078	0.0107	0.0097	0.0090	0.008
	LRVE	0.0120	0.0110	0.0102	0.0089	0.0098	0.0089	0.0083	0.0078	0.0107	0.0097	0.0090	0.008
	Tamura	0.0117	0.0107	0.0099	0.0087	0.0105	0.0096	0.0089	0.0083	0.011	0.0101	0.0093	0.0082

Table 2. Validation of twisting function $f_2(z)$ for calculating natural frequencies in FG square nanoplates.

a/h	schemes	$f_1(z)$		$f_2(z)$			
		Mode 1	Mode 2	Mode 1	Mode 2	Mode 1	Mode 2
10	Mori-Tanaka [22]	0.0330	0.0609	0.0610	0.0332	0.0634	0.0958
	Voigt	0.0331	0.0610	0.0888	0.0338	0.0646	0.0975
	Reuss	0.0339	0.0627	0.0914	0.0349	0.0667	0.1008
	LRVE	0.0350	0.0653	0.0947	0.0360	0.0687	0.1037
	Tamura	0.0339	0.0627	0.0914	0.0349	0.0667	0.1008
20	Mori-Tanaka [22]	0.0085	0.0161	0.0162	0.0083	0.0161	0.0249
	Voigt	0.0084	0.0163	0.0246	0.0085	0.0164	0.0253
	Reuss	0.0087	0.0167	0.0254	0.0088	0.0170	0.0262
	LRVE	0.0089	0.0173	0.0260	0.0090	0.0175	0.0270
	Tamura	0.0087	0.0167	0.0254	0.0088	0.0170	0.0262

We compared our results with those of Natarajan et al. [22], and Table 1 provides a comprehensive comparison between the natural frequencies obtained in our study and the literature values. This table validates the accuracy of our numerical analysis and demonstrates a close agreement with the literature findings. Furthermore, we examined the influence of various factors, including plate thickness ratio a/h, functional models (power-law, Viola-Tornabene four-parameter, trigonometric), and the nonlocal parameter μ, on the natural frequencies. The robustness of our methodology is confirmed, instilling confidence in the reliability of our results.

Additionally, Table 2 focuses on the assessment of the twisting $f_2(z)$ function, used to determine the natural frequencies of FG square nanoplates. Through the comparison of outcomes for different thickness ratios and homogenization models, Table 2 verifies the accuracy and effectiveness of the $f_2(z)$ function in calculating the natural frequencies of the nanoplates. Together, the validation provided by Table 1 and the examination of the twisting function in Table 2 reinforce the credibility of our numerical analysis and pave the way for future parametric studies to explore the impacts of gradient index, side-to-thickness ratio, and nonlocal parameter.

6.1. Effect of nonlocal parameter (μ) and eigenmode

Figure 2 illustrates the interdependence between natural frequency and eigenmode for an FG nanoplate. As the mode number increases, the surface plot reveals a concurrent rise in both natural frequency and eigenmode. This positive correlation indicates larger vibration modes correspond to higher natural frequencies.

The synchronized increase implies the two variables are intrinsically linked for the nanoplate system. Their codependent relationship emerges from the analytical solution used to model the dynamics. Proper formulation is therefore critical to capture the correct eigenmode-frequency pairing.

Overall, the three-dimensional visualization in Figure 2 provides valuable insight into the coupled behavior of eigenmode and natural frequency. It highlights the need to judiciously select an analytical approach to accurately predict the modal frequencies of FG nanoplates across the spectrum of vibration modes.

Figure 3 presents the correlation between the nonlocal parameter and the natural frequency of an FG nanoplate. The investigation focuses on various volume fraction models and employs the LRVE homogenization model with a material index of $p = 2$.

The interplay between nonlocal interactions and material gradation unveils their coupled influence on the natural frequency behavior of nanoplates. As the nonlocal parameter increases, vibrational frequencies uniformly decline across all volume fraction models studied. This points to the critical role of long-range atomic forces in governing the stiffness and dynamic behavior of the nanoplates.

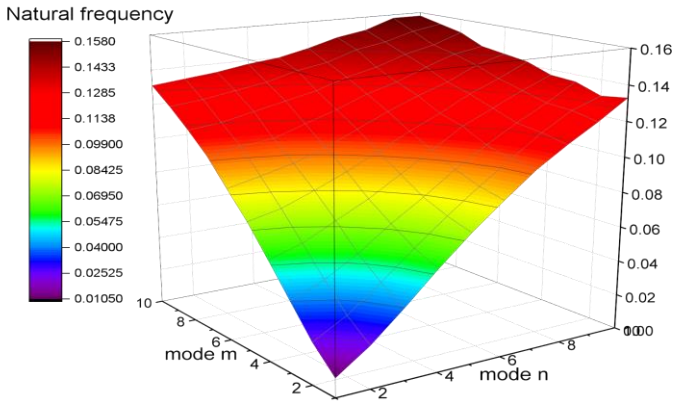

Figure 2: The impact of various modes on the natural frequency of an FG nanoplate through a three-dimensional plot (for the power-law model).

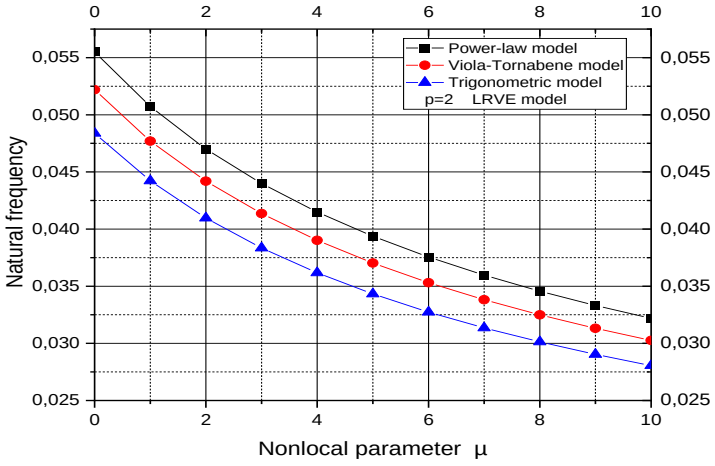

Figure 3: Effect of the nonlocal parameter (μ) and volume fraction models on natural frequency.

With greater nonlocal forces, atomic-level interactions intensify, impeding oscillations and decreasing natural frequencies. The stiffness elevates as atoms feel the effects of their neighbors more strongly. Among the distribution models, the Power-law profile stands out with the highest frequencies, signifying greater stiffness from its graded configuration.

The four-parameter model follows closely behind, while the trigonometric gradation induces the least stiffening and lowest natural frequencies. The results spotlight the subtle interplay between small-scale nonlocal atomic interactions and the larger-scale material gradient. Both factors work in tandem to dictate the emergent dynamic response of the nanoplates.

Figures 4-6 depict the relationship between natural frequencies of an FG nanoplate with a height-to-width ratio of 10 and the first three eigenmode values. The focus is on exploring the impact of different small-scale parameter values, namely the power-law model, Viola-Tornabene four-parameter model, and trigonometric model, on the natural frequencies.

An increase in the nonlocal parameter is observed to lead to a consistent decrease in natural frequencies across all models and modes. This decline indicates the significant influence of small-scale nonlocal forces in governing the stiffness and dynamics of the nanoplate.

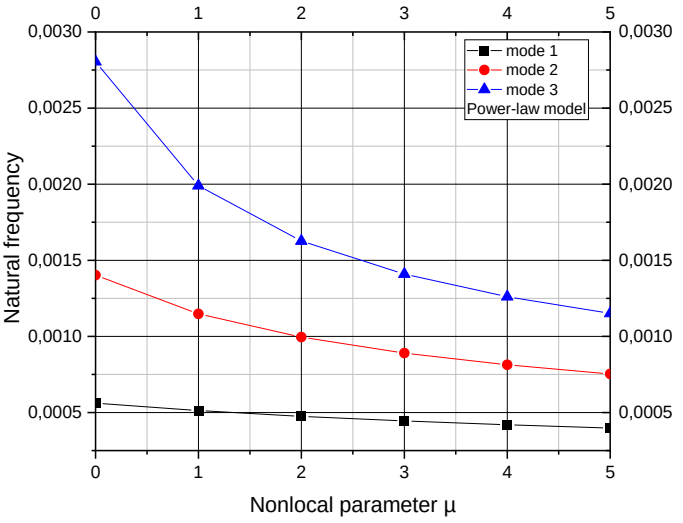

Figure 4: Effect of the nonlocal parameter (μ) and modes on natural frequency for the power-law model.

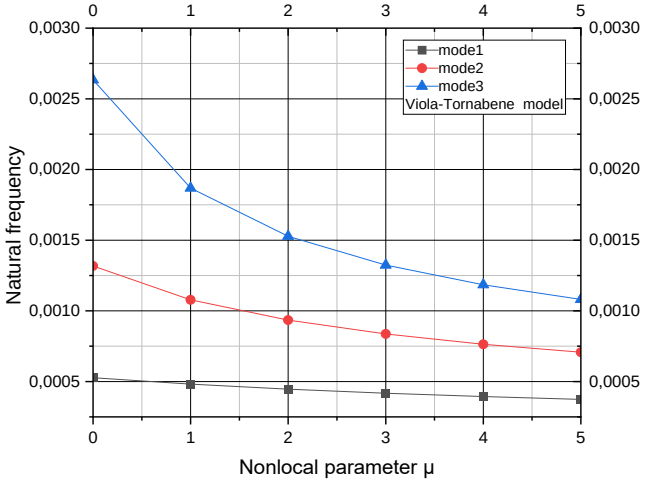

Figure 5: Effect of the nonlocal parameter (μ) and modes on natural frequency for the Viola-Tornabene four-parameter model.

Enhanced nonlocal atomic interactions result in reduced stiffness, leading to impairment of oscillation capacity and lower vibrational frequencies. However, there are notable distinctions between the distribution models. The power-law profile consistently exhibits the highest frequencies, showcasing its superior stiffening ability compared to the four-parameter model, while the trigonometric model lags.

The uniformity across modes emphasizes that the models inherently produce varying stiffness levels regardless of the vibration mode. These results offer a comprehensive understanding of how local atomic-scale forces and longer-range material gradients collaborate to shape the macroscale dynamic characteristics of the nanoplates.

This interconnected perspective is crucial for comprehending and predicting the vibrational properties accurately, achieved through meticulous adjustments of both nonlocal interactions and functional gradation.

6.2. Effect of the aspect ratios (a/h) for different volume fraction models

In Figure 7, the impact of dissimilar volume fraction models on the natural frequency of an FG nanoplate is shown at various aspect ratios (a/h). The analysis is conducted using the LRVE homogenization model with a material index of $p = 2$ and a nonlocal parameter value of $\mu = 1$.

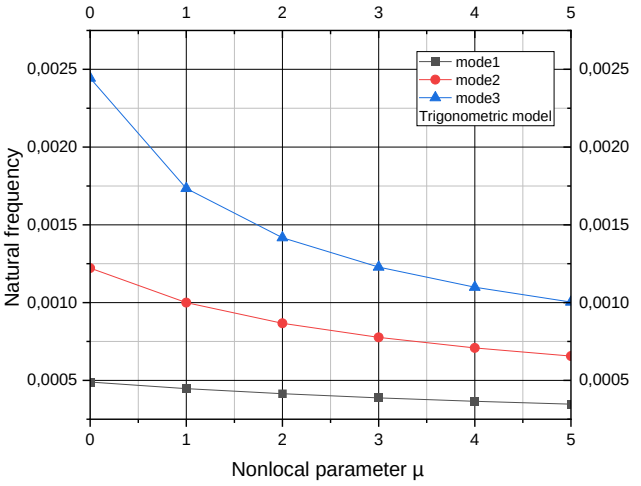

Figure 6: Effect of the nonlocal parameter (μ) and modes on natural frequency for the trigonometric model.

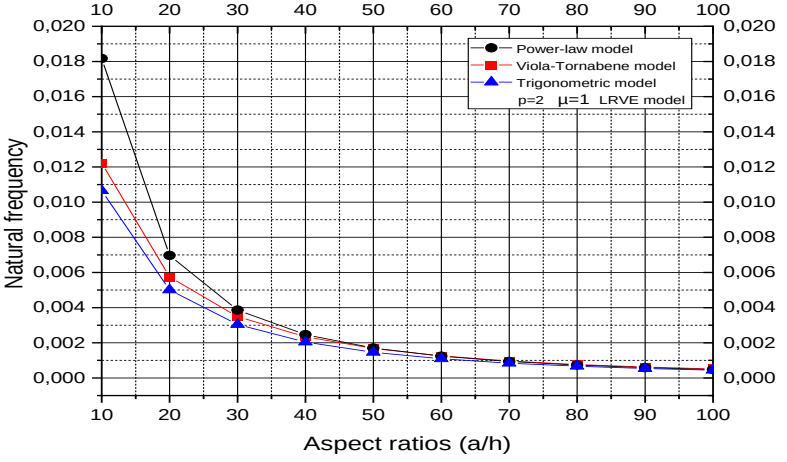

Figure 7: Effect of the aspect ratios (a/h) for different models on the natural frequency

Natural frequency of FG nanoplate decreases as aspect ratio (a/h) decreases, indicating a decrease in stiffness. At lower aspect ratios, the volume fraction models have varying effects on the natural frequency. The power-law model exhibits the highest natural frequency values, followed by the Viola-Tornabene four-parameter model, while the Trigonometric model has the lowest values. However, as the aspect ratio increases, the natural frequency becomes more consistent and approaches a constant value, especially at higher aspect ratios. In summary, the relationship between the volume fraction models and the natural frequency depends on the aspect ratio. The power-law model yields the highest natural frequencies at lower aspect ratios, while the Trigonometric model yields the lowest. At higher aspect ratios, the natural frequency becomes relatively constant across the models.

6.3. Effect of the index material (p) and eigenmode on the natural frequency

Figure 8 illustrates impact of different volume fraction models on natural frequency of an FG nanoplate at varying index material (p) values. The analysis is performed using the LRVE homogenization model with a nonlocal parameter value of $\mu = 1$.

Figure 8 illustrates how different volume fraction models affect the natural frequency of an FG nanoplate at various index material (p) values. The decrease in frequency is attributed to the reduced stiffness of the nanoplate. Increasing index material (p) values lead to a decrease in natural frequency. The power-law model exhibits the highest natural frequency, followed by the Viola-Tornabene four-parameter model, while the trigonometric model has the lowest values. However, as the index material (p) further increases, the natural frequency becomes the same for the Viola-

Tornabene four-parameter and trigonometric models. It is important to note that Power-law model maintains a distinct natural frequency throughout. In summary, the relationship between the volume fraction models and natural frequency of the FG nanoplate depends on the index material (p) values. The power-law model consistently has the highest frequency, the Viola-Tornabene four-parameter model follows, and the trigonometric model has the lowest values. At higher index material values, the natural frequency becomes equivalent for the Viola-Tornabene four-parameter and trigonometric models, while the power-law model retains its unique natural frequency.

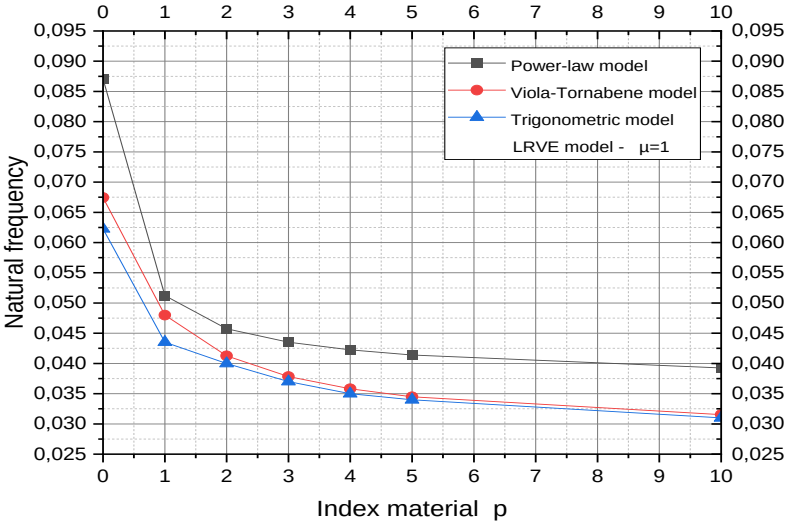

Figure 8: Effect of the index material (p) on the natural frequency

7. Conclusions

This comprehensive study investigated the behavior of functionally graded (FG) nanoplates, providing insights into their characteristics and important design considerations. By examining factors such as homogenization models (Voigt Reuss, LRVE, and Tamura), volume fraction laws (power-law model, Viola-Tornabene four-parameter model, trigonometric model), eigenmode, aspect ratios, index material, and small-scale length parameters, the study evaluated their influence on the natural frequency response of simply supported nanoplates. A novel twisting function was introduced, and its accuracy in predicting natural frequencies in FG square nanoplates was rigorously validated through numerical comparisons with existing literature.

The findings obtained from this research offer valuable guidance for optimizing the design of FG nanoplates. The results affirmed the influence of factors such as thickness ratio, homogenization models, volume fraction laws, nonlocal parameter, eigenmode, aspect ratios, and index material on the natural frequency of the nanoplates. By considering the appropriate homogenization model, volume fraction law, and other identified factors, engineers and researchers can make informed decisions to enhance the natural frequency response of FG nanoplates. Overall, this research significantly contributes to advancing our understanding of FG nanoplate dynamics and their practical applications in various fields, including aerospace, automotive, biomedical, and energy industries.

Funding

This research received no specific grant from any funding agency in the public, commercial, or not-for-profit sectors.

Conflict of Interests

The authors declare that there is no conflict of interest.

References

[1] F. Yang, A. C. M. Chong, D. C. C. Lam, P. Tong, Couple stress based strain gradient theory for elasticity, *International Journal of Solids and Structures,* Vol. 39, pp. 2731-2743, 05/01, 2002.

[2] E. C. Aifantis, Strain gradient interpretation of size effects, *International Journal of Fracture,* Vol. 95, No. 1, pp. 299-314, 1999/01/01, 1999.

[3] H. Moosavi, M. Mohammadi, A. Farajpour, S. Shahidi, Vibration analysis of nanorings using nonlocal continuum mechanics and shear deformable ring theory, *Physica E: Low-dimensional Systems and Nanostructures*, Vol. 44, No. 1, pp. 135-140, 2011.

[4] M. Khorasani, Z. Soleimani Javid, E. Arshid, L. Lampani, Ö. Civalek, Thermo-elastic buckling of honeycomb micro plates integrated with FG-GNPs reinforced Epoxy skins with stretching effect, *Composite Structures*, Vol. 258, pp. 113430, 02/01, 2021.

[5] B. Akgöz, Ö. Civalek, Buckling Analysis of Functionally Graded Tapered Microbeams via Rayleigh–Ritz Method, *Mathematics*, Vol. 10, pp. 4429, 11/24, 2022.

[6] B. Akgöz, Ö. Civalek, Application of strain gradient elasticity theory for buckling analysis of protein microtubules, *Current Applied Physics*, Vol. 11, No. 5, pp. 1133-1138, 2011.

[7] P. Lu, L. He, H. Lee, C. Lu, Thin plate theory including surface effects, *International Journal of Solids and Structures - INT J SOLIDS STRUCT*, Vol. 43, pp. 4631-4647, 08/01, 2006.

[8] M. Sobhy, A comprehensive study on FGM nanoplates embedded in an elastic medium, *Composite Structures*, Vol. 134, 09/01, 2015.

[9] M. Sobhy, A. Radwan, A New Quasi 3D Nonlocal Plate Theory for Vibration and Buckling of FGM Nanoplates, *International Journal of Applied Mechanics*, Vol. 09, pp. 1750008, 02/08, 2017.

[10] A. Zenkour, A novel mixed nonlocal elasticity theory for thermoelastic vibration of nanoplates, *Composite Structures*, Vol. 185, 11/01, 2017.

[11] A. Abdelrahman, M. A. Eltaher, On bending and buckling responses of perforated nanobeams including surface energy for different beams theories, *Engineering with Computers*, Vol. 38, pp. 1-27, 06/01, 2022.

[12] Q.-H. Pham, T. T. Tran, V. K. Tran, P.-C. Nguyen, T. Nguyen-Thoi, A. M. Zenkour, Bending and hygro-thermo-mechanical vibration analysis of a functionally graded porous sandwich nanoshell resting on elastic foundation, *Mechanics of Advanced Materials and Structures*, Vol. 29, No. 27, pp. 5885-5905, 2022.

[13] A. Garg, H. D. Chalak, A. Zenkour, M.-O. Belarbi, M. S. A. Houari, A Review of Available Theories and Methodologies for the Analysis of Nano Isotropic, Nano Functionally Graded, and CNT Reinforced Nanocomposite Structures, *Archives of Computational Methods in Engineering*, 10/04, 2021.

[14] P. Phung-Van, C. H. Thai, A novel size-dependent nonlocal strain gradient isogeometric model for functionally graded carbon nanotube-reinforced composite nanoplates, *Engineering with Computers*, pp. 1-14, 2021.

[15] A. Zenkour, R. Alghanmi, A refined quasi-3D theory for the bending of functionally graded porous sandwich plates resting on elastic foundations, *Thin-Walled Structures*, Vol. 181, pp. 110047, 12/01, 2022.

[16] M. Arefi, S. Firouzeh, E. Mohammad-Rezaei Bidgoli, Ö. Civalek, Analysis of Porous Micro-plates Reinforced with FG-GNPs Based on Reddy plate Theory, *Composite Structures*, Vol. 247, pp. 112391, 04/01, 2020.

[17] A. Garg, H. D. Chalak, A. Zenkour, M.-O. Belarbi, R. Sahoo, Bending and free vibration analysis of symmetric and unsymmetric functionally graded CNT reinforced sandwich beams containing softcore, *Thin-Walled Structures*, Vol. 170, pp. 108626, 01/01, 2022.

[18] İ. Esen, A. Abdelrahman, M. A. Eltaher, Free vibration and buckling stability of FG nanobeams exposed to magnetic and thermal fields, *Engineering with Computers*, Vol. 38, 08/01, 2022.

[19] L. Hoa, P. Vinh, N. Duc, T. Nguyen-Thoi, L. Son, D. Thom, Bending and free vibration analyses of functionally graded material nanoplates via a novel nonlocal single variable shear deformation plate theory, *Proceedings of the Institution of Mechanical Engineers, Part C: Journal of Mechanical Engineering Science*, Vol. 235, pp. 095440622096452, 10/15, 2020.

[20] Ş. Akbaş, Modal analysis of viscoelastic nanorods under an axially harmonic load, *Advances in nano research*, Vol. 8, pp. 277-282, 05/27, 2020.

[21] E. E. Ghandourh, A. M. Abdraboh, Dynamic analysis of functionally graded nonlocal nanobeam with different porosity models, *Steel and Composite Structures, An International Journal*, Vol. 36, No. 3, pp. 293-305, 2020.

[22] S. Natarajan, S. Chakraborty, M. Thangavel, S. Bordas, T. Rabczuk, Size-dependent free flexural vibration behavior of functionally graded nanoplates, *Computational Materials Science*, Vol. 65, pp. 74-80, 2012.

[23] M. Koizumi, FGM activities in Japan, *Composites Part B: Engineering*, Vol. 28, No. 1, pp. 1-4, 1997/01/01/, 1997.

[24] H.-T. Thai, T. P. Vo, A nonlocal sinusoidal shear deformation beam theory with application to bending, buckling, and vibration of nanobeams, *International Journal of Engineering Science*, Vol. 54, pp. 58-66, 2012.

[25] F. Ebrahimi, M. Barati, A. Zenkour, Vibration Analysis of Smart Embedded Shear Deformable Nonhomogeneous Piezoelectric Nanoscale Beams based on Nonlocal Elasticity Theory, *International Journal of Aeronautical and Space Sciences,* Vol. 18, pp. 255-269, 06/01, 2017.

[26] A. Shariati, D. w. Jung, H. Mohammad-Sedighi, K. K. Żur, M. Habibi, M. Safa, On the Vibrations and Stability of Moving Viscoelastic Axially Functionally Graded Nanobeams, *Materials,* Vol. 13, No. 7, pp. 1707, 2020.

[27] J. Reddy, Nonlocal theories for bending, buckling and vibration of beams, *International Journal of Engineering Science,* Vol. 45, pp. 288-307, 02/01, 2007.

[28] J. Reddy, S. Pang, Nonlocal continuum theories of beams for the analysis of carbon nanotubes, *Journal of Applied Physics,* Vol. 103, pp. 023511-023511, 02/01, 2008.

[29] M. A. Eltaher, S. Emam, F. Ibrahim, Free vibration analysis of functionally graded size-dependent nanobeams, *Applied Mathematics and Computation,* Vol. 218, pp. 7406-7420, 03/01, 2012.

[30] R. Nazemnezhad, S. Hosseini-Hashemi, Nonlocal nonlinear free vibration of functionally graded nanobeams, *Composite Structures,* Vol. 110, pp. 192-199, 04/01, 2014.

[31] F. Ebrahimi, M. Barati, Ö. Civalek, Application of Chebyshev–Ritz method for static stability and vibration analysis of nonlocal microstructure-dependent nanostructures, *Engineering with Computers,* Vol. 36, 07/01, 2020.

[32] L. Hadji, M. Avcar, Nonlocal free vibration analysis of porous FG nanobeams using hyperbolic shear deformation beam theory, *Advances in Nano Research,* Vol. 10, pp. 281-293, 03/16, 2021.

[33] Y. Gafour, A. Hamidi, A. Benahmed, M. Zidour, T. Bensattalah, Porosity-dependent free vibration analysis of FG nanobeam using non-local shear deformation and energy principle, *Advances in nano research,* Vol. 8, No. 1, pp. 37-47, 2020.

[34] A. C. Eringen, Theory of micropolar plates, *Zeitschrift für angewandte Mathematik und Physik ZAMP,* Vol. 18, pp. 12-30, 1967.

[35] A. C. Eringen, Nonlocal polar elastic continua, *International journal of engineering science,* Vol. 10, No. 1, pp. 1-16, 1972.

[36] A. C. Eringen, D. Edelen, On nonlocal elasticity, *International journal of engineering science,* Vol. 10, No. 3, pp. 233-248, 1972.

[37] A. C. Eringen, On differential equations of nonlocal elasticity and solutions of screw dislocation and surface waves, *Journal of applied physics,* Vol. 54, No. 9, pp. 4703-4710, 1983.

[38] B. Farshi, A. Assadi, A. Alinia-ziazi, Frequency analysis of nanotubes with consideration of surface effects, *Applied Physics Letters,* Vol. 96, pp. 093105-093105, 03/02, 2010.

[39] R. Billel, Contribution to study the effect of (Reuss, LRVE, Tamura) models on the axial and shear stress of sandwich FGM plate (Ti–6A1–4V/ZrO2) subjected on linear and nonlinear thermal loads, *AIMS Materials Science,* Vol. 10, No. 1, pp. 26-39, 2023.

[40] B. Rebai, K. Mansouri, M. Chitour, A. Berkia, T. Messas, F. Khadraoui, B. Litouche, Effect of idealization models on deflection of functionally graded material (FGM) plate, *Journal of Nano-and Electronic Physics,* Vol. 15, No. 1, 2023.

[41] W. Voigt, Ueber die Beziehung zwischen den beiden Elasticitätsconstanten isotroper Körper, *Annalen der physik,* Vol. 274, No. 12, pp. 573-587, 1889.

[42] A. Reuß, Berechnung der fließgrenze von mischkristallen auf grund der plastizitätsbedingung für einkristalle, *ZAMM-Journal of Applied Mathematics and Mechanics/Zeitschrift für Angewandte Mathematik und Mechanik,* Vol. 9, No. 1, pp. 49-58, 1929.

[43] M. M. Gasik, R. R. Lilius, Evaluation of properties of W□ Cu functional gradient materials by micromechanical model, *Computational materials science,* Vol. 3, No. 1, pp. 41-49, 1994.

[44] J. R. Zuiker, Functionally graded materials: choice of micromechanics model and limitations in property variation, *Composites Engineering,* Vol. 5, No. 7, pp. 807-819, 1995.

[45] I. Tamura, Strength and ductility of Fe-Ni-C alloys composed of austenite and martensite with various strength, in *Proceeding of,* Cambridge, Institute of Metals, pp. 611-615.

[46] T. Mori, K. Tanaka, Average stress in matrix and average elastic energy of materials with misfitting inclusions, *Acta metallurgica,* Vol. 21, No. 5, pp. 571-574, 1973.